

# Modelling and Understanding of Chatter

P.Wolfrum<sup>1</sup>    A.Gepperth<sup>1</sup>    Y.Sandamirskaya<sup>1</sup>  
O.Webber<sup>2</sup>    N.Raabe<sup>3</sup>    G.Szepannek<sup>3</sup>    G.Schoener<sup>1</sup>

Februar 2006

<sup>1</sup>Institut für Neuroinformatik, Universität Bochum, D-44801 Bochum

<sup>2</sup>Institut für Spanende Fertigung, Universität Dortmund, D-44227  
Dortmund

<sup>3</sup>Fachbereich Statistik, Universität Dortmund, D-44221 Dortmund

**Abstract.** Recent analysis in chatter modelling of BTA deep-hole drilling consisted in phenomenological modelisation of relationships between the observed time series and appearance of chatter during the process. Using the newly developed MEWMA control chart [4, 5], it has even been possible to predict the occurrence of chatter about 30 to 50 mm in advance (i.e. up to one minute before the chatter starts).

Unfortunately, no relationships between the machine and model parameters have been detected. Therefore, in this paper a physical model of the boring bar is taken into account. Simulation studies of the regenerative process are performed. These simulated time series show the same characteristics as the data recorded during the drilling process and thus support the validity of our model. By running such simulations, we intend to find strategies for chatter prevention in future work.

# 1 Introduction

## 1.1 Deep-Hole Drilling

In metal cutting one speaks of deep-hole drilling, when for the proportion of length  $l$  to diameter  $D$  of the hole to be machined,  $l/D \geq 3$  holds. When the diameter  $D$  exceeds 20mm typically the BTA deep-hole drilling process is applied. BTA stands for ‘Boring and Trepaning Association’. This refers to the design of the tool which is shown in Figure 1. The special construction of this tool leads to long holes with very smooth walls and a high degree of straightness. In many cases the BTA deep-hole drilling process is the final step in the production of expensive workpieces. For example axial bores in turbines or compressor shafts are produced with this process. It is extremely important to avoid dynamic disturbances in the process because such disturbances can mean high financial losses.

The machine tool used in the experiments, its components, and the process parameters are described in the next subsections. In the following subsection the tool and the general principal of BTA deep-hole drilling are described.

## 1.2 The Machine Tool

The machine tool has six main components: two drive units for the rotary motion of the workpiece and the rotary and translation motion of the tool, the machine bed, the oil supply device containing the starting bush, the damper, and the tool – boring bar assembly.

A peculiarity of the BTA deep-hole drilling process is that the the tool and the workpiece may be driven. This means that drilling can be performed in three different ways:

1. Turning tool and standing workpiece;
2. Standing tool and turning workpiece;
3. Turning tool and workpiece in opposite directions.

The following parameters can be influenced on the machine:

- The axial feed  $f$  in  $mm/rev$

- The cutting velocity (cutting speed)  $v_c$  in  $m/min$
- The flow rate of the oil  $\dot{V}$  in  $l/min$
- The position of the damper
- The operating pressure of the damper

The *cutting velocity* is automatically controlled and therefore is not exactly on target in the modelling process. It is taken into account by measuring the true number of revolutions per second which then allows the effect of the variation in this parameter to be inferred.

The *axial feed* influences the speed of the boring substantially, since it determines the thickness of the chips which are removed by the cutting edge.

The *flow rate of the oil* determines the speed of transportation of the chips from the cutting edge and the cooling and lubrication of the process. It also influences the damping properties of the whole assembly.

The *damper* serves to prevent dynamic disturbances (see section 1.4) and to this aim it can be positioned along the boring bar. Its position can be fixed on the machine bed or relative to the drive unit of the tool. The pressure, with which the damper is clamped to the boring bar, is determined by the machine operator. If the operator detects a disturbance (by sound or vibrations felt on the boring bar) he/she can vary the position and the pressure until the disturbance disappears.

### 1.3 Principle of the BTA Deep-Hole Drilling

The BTA tool has only one cutting edge and two or three guiding pads. This is illustrated in Figure 1. The chips are transported away by the cutting fluid via the chip mouth and through the boring bar. The asymmetrical geometry of the tool leads to forces pushing outwards against the walls of the hole. These forces are counteracted by reactive forces at the guiding pads. The tool is thereby guided in the machined hole and at the same time the bored hole walls are smoothed. Since the chips are transported within the boring bar they cannot damage the hole surface, and hence a high quality of the holes can be achieved.

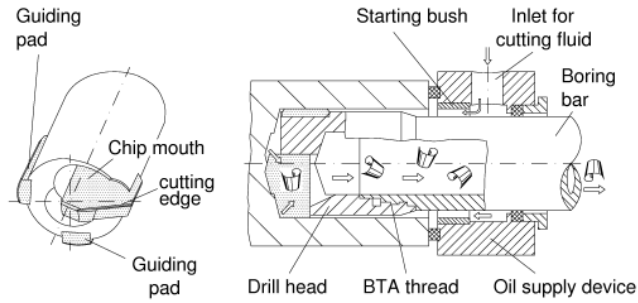


Figure 1: Boring tool and details of the working principle.

## 1.4 Chatter Vibrations

The main aim of the project is to find a way to deal with two dynamic disturbances (chatter vibration and spiralling, see Figure 2) and more precisely, to predict their occurrence and prevent them by appropriate controls.

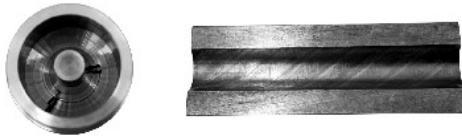


Figure 2: Radial chatter marks on the bottom of the bore hole (left) and effects of spiralling on the bore hole wall (right).

In this paper, a model is proposed to simulate the phenomenon of chatter during the process. Therefore this phenomenon is briefly described here. As the name suggests, this disturbance is audible. The acoustic effect that accompanies chatter vibration can best be described as a high-pitched tone which occurs during the process. The tone suggests regularly interrupted cutting. A sawtooth pattern is produced at the bottom of the hole (Figure 2, on the left). Chatter leads to significantly increased wear of the cutting edges and in more extreme cases it leaves so-called chatter marks on the hole surface.

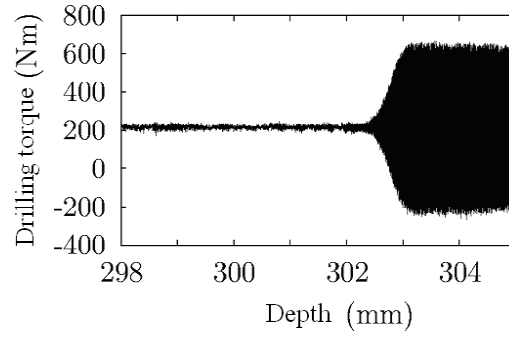


Figure 3: Exemplary time series of the drilling torque with occurrence of chatter.

Having observed out-of-phase torsional and longitudinal vibration during chatter, Thai (1983) traced this type of behavior of the BTA deep-hole drilling process back to the principle of coupled states. Furthermore, from the high dynamic content of the process torque, he inferred that the cutting parts periodically disengage from the workpiece when there is chatter vibration.

## 2 Background for regenerative chatter analysis

Chatter in turning or cutting is usually assumed to be a regenerative process (there exist also other explanations like thermoplastic changes in the material). Because of external perturbation, tool starts an oscillation relative to workpiece, producing a wavy surface. Therefore, the chip thickness that has to be cut in the next round will also vary. Since cutting force depends on the area of the chip ( $F = f(A)$ ) and therefore on its thickness  $\Delta h$  (breadth is usually constant), cutting force is a function of the current and by one round delayed relative positions of tool and workpiece. Consequently, cutting force also varies.

In processes like cutting and turning the vibrations that produce the varying cutting force are orthogonal to the rotation. There need to be no oscillations in the direction of rotation to generate chatter. Therefore the delay can be assumed to be the constant rotation time  $T$  of the process.

For the drilling process this is not the case, which can be seen as follows. The chip thickness of the process is the offset of the tool between two rotations in axial direction. We do not assume axial vibrations of the workpiece or tool (it is the best assumption due to high stiffness). Also the feed rate is constant. Therefore the relative displacement after  $T$  is also constant, consequently also the cutting force ( $F = f(\Delta h)$ ), and there can be no regenerative effect producing chatter. This holds if we assume that  $F \neq f(\dot{\phi})$ , which is the usual assumption.

However, chatter can be explained if we take into account the varying rotation time  $T = T_0 + \delta t$ . The varying  $T$  results directly from the assumed rotational vibrations. For an increased  $T$  (thus a slower rotation speed), the tool has moved a bigger  $\Delta h$  since the last rotation, leading to a bigger cutting force (and corresponding moment). This will slow down the tool even more, until the restoring forces within the bar become too strong. The argument works the same for a decreased  $T$ , and so we get a self-exciting vibration. Usually this process will be damped at some point through higher order terms, otherwise it would lead to resonance catastrophe.

So with the assumptions taken above, chatter can only be explained if the varying rotation time is explicitly taken into account. The classic analytical papers like [1] with DDE methods applied, are therefore not directly applicable for us. Since we cannot simply use a delay differential equation

with constant delay  $\delta t$ , analysis becomes harder. To calculate chip thickness we have to use

$$\Delta h(t) = z(t) - z(t(\Phi(t) - 2\pi)). \quad (1)$$

Here  $\Delta h(t)$  is the varying chip thickness,  $z(t)$  is the coordinate in the boring direction and  $\Phi(t)$  is the total rotation angle of the tool from the beginning of the process. The (1) can only be written in closed form, if we define the inverse function

$$f(\phi, t) = \max_{\tau} \{\tau : \tau < t, \Phi(\tau) = \phi\}. \quad (2)$$

Then

$$\Delta h(t) = z(t) - z(f(\Phi(t), t)). \quad (3)$$

The maximum operator is only necessary if we assume that the tool can vibrate so strongly that it leaves the work piece. Due to difficulties in analytical predictions for the system with varying delay, analysis by simulation experiments was held.

A good introduction to the subject may be found in [9]. More advanced analytical considerations are developed in [1] and [8].

### 3 Deriving motion equations for a bar as a multibody system

Initially the bar (parametrized by its axial coordinate  $z$ ) is assumed to be a continuous body, whose dynamics is determined by the moments which act on the bar. Moments are the sum of external moments (motor forces and friction) and internal moments from the neighboring infinitesimal bar elements. Let  $\phi(z, t)$  describe the angular deviation of the bar from its resting position. The theory of torsional deformations gives the equation of motion

$$\rho J_p \frac{\partial^2}{\partial t^2} \phi(z, t) = \sum \frac{\partial}{\partial z} M(z, t) = \sum \frac{\partial}{\partial z} (M_T(z, t) + M_F(z, t) + M_{ext}(z, t)), \quad (4)$$

where all the moments are in radial direction and  $M_T, M_F$  denote the moments caused by the torsion of the bar and friction, respectively.  $M_{ext}$  stands for the moment caused by the drill-workpiece interaction which is defined by the trespassing force model, described in the section 5.

In particular, friction is assumed to be viscose, i.e. proportional to the angular velocity:  $M_F = \mathcal{F}(z, t)\dot{\phi}(z, t)$ . The density of the boring bar and its moment of inertia per unit area perpendicular to its axis are denoted by  $\rho$  and  $J_p$ . We use dots to indicate time derivatives and primes to indicate space derivatives.

Replacing the torsional moment by Hooke's law, we obtain  $M_T = GJ_T\phi'(z, t)$ .  $G$  is the shear modulus of the bar and  $J_T$  its torsional moment of inertia. This gives us the following equation of motion for the torsional moments alone:

$$\begin{aligned}\ddot{\phi}(z, t) &= c^2\phi''(z, t), \\ c^2 &= \frac{GJ_T}{\mu J_p}.\end{aligned}\tag{5}$$

For a circular bar as considered here, it can be shown that  $J_p = J_T$  which simplifies the preceding equation. Inserting all this into equation (4), we obtain

$$\mu J_p \ddot{\phi} = GJ_T\phi''(z, t) + \mathcal{F}'(z, t)\dot{\phi}(z, t) + M'_{ext}(z, t).\tag{6}$$

To run a simulation, this equation has to be discretized in space. The bar is discretized into  $K$  pieces with the behaviour of the pieces determined by their equations of motion. The leftmost piece (containing the drill head) is assigned the index 0, whereas the rightmost piece has index  $K - 1$ . We thus assume a bar consisting of  $K$  pieces of length  $\Delta z$ .  $\phi(z, t)$  becomes a vector  $\vec{\phi}(t)$  containing the angle positions of the  $K$  pieces. Thus we have a system of  $K$  differential equations. By discretizing the spatial derivatives, we find

$$\begin{aligned}\mu J_p \ddot{\phi}_i &= \frac{GJ_T}{(\Delta z)^2}[(\phi_{i+1}(t) - \phi_i(t)) + \phi_{i-1}(t) - \phi_i(t)] + \\ &+ \mathcal{F}'_i(t)\dot{\phi}_i(t) + M'_{ext,i}(t) = \\ &= \frac{GJ_T}{(\Delta z)^2}[\phi_{i+1}(t) + \phi_{i-1}(t) - 2\phi_i(t)] + \frac{f_i(t)}{\Delta z}\dot{\phi}_i(t) + \frac{m_{ext,i}}{\Delta z}(t).\end{aligned}\tag{7}$$

The discretized external moment  $\vec{M}_{ext}$  acts on the leftmost element only: when using a backward derivative approximation, only the last element of  $m_{ext}$  contains a nonzero value. Due to the complicated nature of frictional interactions, an intuitive and simple expression for  $\vec{F}(t)$  cannot be given.



Instead, a pragmatic approach is used. Having so far simplified the equations of motions to

$$M\ddot{\vec{\phi}}(t) = P\vec{\phi}(t) + F\dot{\vec{\phi}} + \vec{m}_{ext}(t), \quad (8)$$

where  $M, P$  and  $F$  are called the mass, stiffness and friction matrices, respectively, we suppose  $F = \alpha M + \beta C + \gamma P$ . Since all discretized bar elements have the same moment of inertia in our model,  $M = \mu J_p I_{K \times K}$ .  $C$  represents the friction caused by the stuffing box:  $C = \text{diag}(0, \dots, 1, 0, \dots)$ . Thus the diagonal of  $C$  has a nonzero element at the bar element(s) having contact with the stuffing box. For practical reasons,  $C$  is interpolated: if only one bar element has contact with the stuffing box, the unit value is "distributed" over adjacent bar elements. The values of  $\alpha, \beta$  and  $\gamma$  are determined from fitting this model to experimental data. Experiments have shown that  $\gamma$  is close to zero. It is therefore disregarded in the following considerations.

Boundary conditions must be taken into account: the left end of the boring bar is free, therefore interaction with the next discretized element does not exist; equally, the right end of the bar is fixed, therefore  $\phi$  and all its derivatives are zero. Here, the  $K \times K$ -matrices  $F$  and  $P$  are defined as

$$F = -\frac{1}{\Delta z} \text{diag}(\alpha, \alpha, \dots, \alpha + \beta, \alpha, \dots), \quad (9)$$

$$P = -\frac{GJ_T}{(\Delta z)^2} \begin{pmatrix} -1 & 1 & 0 & \dots & 0 \\ 1 & -2 & 1 & \dots & \vdots \\ 0 & \ddots & \ddots & \ddots & 0 \\ \vdots & 0 & 1 & -2 & 1 \\ 0 & 0 & \dots & 0 & 0 \end{pmatrix}. \quad (10)$$

For reasons of computational efficiency it makes sense to rewrite equation (8) in a form using the new variable

$$\vec{x} = \begin{pmatrix} \vec{\phi} \\ \dot{\vec{\phi}} \end{pmatrix}, \quad (11)$$

where  $\vec{\phi} = (\phi_1, \dots, \phi_K)^T$ ,  $\dot{\vec{\phi}} = (\dot{\phi}_1, \dots, \dot{\phi}_K)^T$ .

Thus, after trivial transformations, the model can be written as follows:

$$\dot{\vec{x}} = \begin{pmatrix} A_{11} & A_{12} \\ A_{21} & A_{22} \end{pmatrix} \vec{x} + \begin{pmatrix} 0 \\ \vec{M}_{ext} \end{pmatrix} = \begin{pmatrix} 0 & I_K \\ P & F \end{pmatrix} \vec{x} + \frac{m_{ext}}{\mu J_p \Delta z} \begin{pmatrix} 0 \\ \vec{e}_0 \end{pmatrix}. \quad (12)$$

Here the conditions  $\mathbf{A}_{12} + \mathbf{A}_{22} - \mathbf{I}_k = \mathbf{F}$  and  $\mathbf{A}_{11} + \mathbf{A}_{21} = \mathbf{P}$  must hold if the new equations of motion are to be equivalent to (8).  $\mathbf{I}_{K \times K}$  denotes a unit matrix of dimension  $K$ ,  $\vec{e}_i$  is the  $i$ -th unit vector of dimension  $K$  with elements  $e_{ij} = \delta_{ij}$ . The boundary conditions are taken into account in the matrix  $\mathbf{P}$ : We assume the right end to be fixed, so the first and the second derivatives are 0 there and thus the  $K^{\text{th}}$  row of  $\mathbf{P}$  is filled with zeros. On the left side of the instrument we have an open end, so no influence from an element to the left occurs here, which is considered in the first row of the matrix  $\mathbf{P}$ .

We get a contribution from the cutting force  $m_{ext}$  exerted by the drill-workpiece interaction on the left side of the instrument. The details of this interaction are subject of the trepanning force model and described in section 5. The upper part of the external moment term in the right-hand side of equation (12) is zero because a moment can only be coupled to the second derivatives of  $\vec{\phi}$ .

Additive noise enters via the trepanning force model. Thus, (12) represents a coupled system of  $2K$  time differential equations that we can simulate.

## 4 Integration methods

A fourth order Runge-Kutta method is used for the simulation of the coupled system (12). For details of the algorithm, please see [7]. The simulation is computationally expensive, a run of 300 simulated seconds takes about 10 minutes of processing time on a 3Ghz machine.

Integrating stochastic processes correctly is non-trivial (see, e.g. [2]). In [6], a second order method is proposed which works as follows (not considering the noise terms). Assuming

$$k_1 = f(y, t),$$

the difference  $\Delta y$  is calculated as

$$\Delta y = \frac{h}{2}(k_1 + f(y + hk_1, t + h)).$$

The classical RK method suggests:

$$\Delta y = hf\left(y + \frac{h}{2}k_1, t + \frac{h}{2}\right).$$

Experiments showed that the method from [6] performed poorer than Runge-Kutta methods (from the point of view of accuracy and numerical stability). Since we do not simulate a clearly defined stochastic process anyway, the following method was employed for dealing with random noise using the Runge-Kutta method. Noise is added after each integration step, not after every interpolation point. Noise is scaled with  $\sqrt{h}$ . Furthermore, noise is only added to the *acceleration* of the bar, not its velocity. It must be also taken care not to add noise to the right-hand end of the bar which should stay fixed.

## 5 Modeling of the regenerative process

Based on experiments, a working point moment of 400Nm is assumed. To this, a term linear in the deviation of the chip size is added. A purely linear function of chip thickness  $m_{ext} = k * \Delta h$  is not sufficient, but if the deviational moment factor  $k_d$  is about 2 orders of magnitude bigger than the proportional factor  $k_0$  leading to the working point moment, this can lead to regenerative chatter. This is a plausible assumption since in the literature the deviational influences are usually assumed to be of higher order (see [9], p.742).

This purely linear deviational term leads to resonance catastrophe. By restricting the magnitude of this term from above, we can get a self-stabilized chatter process. Therefore, in the current form the model is determined by two parameters: the slope of the linear term  $k$  and the upper bound  $b$  on the linear model.

The onset of chatter is very sensitive to initial conditions. Since we want to study how chatter develops in the running process operating at working point, we need to make sure that the process is in the working point state from the beginning. This can either be done by starting it with  $x_0 = 0$  and  $M_{wp} = 0$ , or by setting  $x_0$  equals the working point value of a given  $M_{wp}$ . In the first case, chatter does not start so easily. Using the same parameters as usual, it will start later.

**Acknowledgment.** This work has been supported by the Collaborative Research Center ‘Reduction of Complexity in Multivariate Data Structures’ (SFB 475) of the German Research Foundation (DFG).

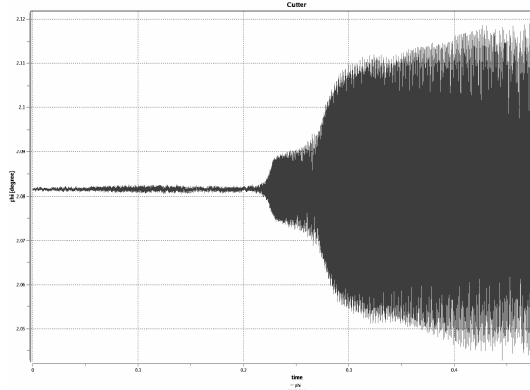


Figure 4: Simulated process with chatter.

## References

- [1] ALTINTAS, Y., and WECK, M. (2004): Chatter Stability of Metal Cutting and Grinding. *Annals of the CIRP*, 53(2), 619–642.
- [2] BURRAGE, K. , BURRAGE, P., and MITSUI, T. (2000): Numerical solutions of stochastic differential equations. implementation and stability issues. *Journal of Computational and Applied Mathematics*, 125(1-2):171–182.
- [3] LATINOVIC, V., and OSMAN, M. (1989): Optimal Design of BTA Deep-hole Cutting Tools with Staggered Cutters. *International Journal of Production and Research*, 27(1), 153–173.
- [4] MESSAOUD, A., THEIS, W., WEIHS, C., HERING, F. (2005): Application and use of multivariate control charts in a BTA deep hole drilling process, *In: C. Weihs, W. Gaul: Classification- The Ubiquitous Challenge*; Springer Studies in Classification, pp.648-655.
- [5] MESSAOUD, A., WEIHS, C., HERING, F. (2005): Time Series, Control Charts: An Industrial application, *Proceedings of AMSDA 2005, Brest*.
- [6] MILSHTEIN, A. (1976): A method of second-order accuracy integration of stochastic differential equations. *Theory Probab. Appl.*, 23:396–401.

- [7] PRESS, H., FLANNERY, B., TEUKOLSKY, S., and VETTERLING, W. (1992):. *Numerical Recipes: The Art of Scientific Computing*. Cambridge University Press, Cambridge (UK) and New York, 2nd edition.
- [8] STEPAN, G. (1998): Delay-Differential Equation For Machine Tool Chatter, *In: Moon, F.: Dynamics and Chaos in Manufacturing Processes*, John Wiley and Sons, New York.
- [9] STEPAN, G. (2001): Modelling nonlinear regenerative effects in metal cutting. *Philosophical Transactions: Mathematical, Physical and Engineering Sciences*, 359(1781):739 – 757.
- [10] THAI, T. (1983): *Beitrag zur Untersuchung der selbsterregten Schwingungen von Tiefbohrwerkzeugen*, PhD thesis, Universität Dortmund.
- [11] VDI (1974): VDI-Richtlinie 3210: Tiefbohrverfahren. *VDI Düsseldorf*.